Characterization of a Virtual Air Gap

Jean-François Brudny, Guillaume Parent, Inès Naceur

▶ **To cite this version:**

Jean-François Brudny, Guillaume Parent, Inès Naceur. Characterization of a Virtual Air Gap. XVII International Symposium on Electromagnetic Fields (ISEF), Sep 2014, Valencia, Spain. hal-04114214

HAL Id: hal-04114214
https://hal.science/hal-04114214v1

Submitted on 26 Oct 2023

HAL is a multi-disciplinary open access archive for the deposit and dissemination of scientific research documents, whether they are published or not. The documents may come from teaching and research institutions in France or abroad, or from public or private research centers.

L'archive ouverte pluridisciplinaire **HAL**, est destinée au dépôt et à la diffusion de documents scientifiques de niveau recherche, publiés ou non, émanant des établissements d'enseignement et de recherche français ou étrangers, des laboratoires publics ou privés.

ISEF 2015 - XVII International Symposium on Electromagnetic Fields
in Mechatronics, Electrical and Electronic Engineering

Valencia, Spain, September 10-12, 2015

CHARACTERIZATION OF A VIRTUAL AIR GAP

Jean-François Brudny[1], Guillaume Parent[1] and Inès Naceur[2]

[1]Univ. Artois, EA 4025, Laboratoire Systèmes Electrotechniques et Environnement (LSEE), Béthune, F-62400, France

[2]SATT Nord, F-59800 Lille, France

Abstract* – *This paper deals with an analytical model of the virtual air gap function in order to define design rules when this technique is used inside complex devices.

Introduction

The virtual air gap (VAG) concept has been introduced at the end of the 90s in order to control the transformer inrush currents [1]. This technique has been taken up in North America [2,3]. The principle consists in feeding auxiliary windings (AW) located inside a magnetic core (MC) with a DC current in order to generate variable local saturations, allowing to modify the RMC core reluctance. That way, the latter can be assimilated to a regular MC with a mechanical air gap of variable "g" thickness. From the point of view of a main winding (MW) carried by MC and supplied by an AC voltage source, it can also be seen as a modification of its L^p inductance. Due to the complexity of the magnetic phenomena occurring around the AWs, the VAG behavior is usually studied by using Finite Element Analysis (FEA), although investigations were conducted to provide further characterizations [4]. Recently, two patents about the VAG [5,6], involving EDF R&D, as well as a communication on the use of such technique for the protection of a DVR [7], were published. In order to define preliminary design rules, this paper establishes a model to characterize analytically the function provided by this VAG.

First, the studied structure equipped with a VAG is introduced. Then, an analytical modeling is reported. The third part presents the waveforms of several signals characterizing the device, which are deduced from a simple spreadsheet and that allow to formulate the equation representing the behavior of the VAG. Finally, relevant specifications useful for the design of such a device are presented as well as experimental results.

Characterization of a virtual air gap

Fig. 1 presents a MC on which is wound a MW of n^p turns, fed by an i^p current supplied by an AC v^p voltage source at a "f" frequency (period "T", angular frequency "ω"). The MC, whose dimensions (in mm) are also shown in Fig. 1, is made with an isotropic steel characterized by its first magnetization curve allowing to define the evolution of the relative magnetic permeability $\mu_r(b)$ presented in Fig. 2. In that figure, note that for low values of the magnetic flux density the inflexion point has been voluntarily neglected. This MC is characterized by its $S_{MC}=lw$ cross section and its $L_{MC}=L'+h-2w$ mean length. The local saturation of the core is ensured by two AWs of n^A turns each located in four

ISBN: 978-84-606-9102-0

orifices. The geometry of the orifices is presented in Fig. 3 with a=14.5 mm, b=20 mm, c=20 mm, d=4 mm. This specific geometry brings two advantages:

1. during a conventional operating mode, *i.e.* $i^A=0$, it allows to limit the perturbations inside the MC,
2. during a current limiting operating mode, *i.e.* $i^A\neq0$, it allows to limit the Ampere-turns losses produced by this current along the x direction by focusing the magnetic flux lines along the y direction.

n^p and n^A are equal to 252 and 20 respectively. The two AWs are connected in order to produce opposite magnetic phenomena when fed by an i^A DC current. That way, those phenomena cancel each other outside the area, qualified as "disturbed", around the AWs as shown in Fig 4a. Fig. 4b, as for it, shows the distribution of the field lines in this disturbed area for $i^A=20$ A, $V^p=240$ V, f=50 Hz at a time step "t" such that $b^p=\hat{b}^p=0.984T$, leading to $i^p=\hat{i}^p=2.18A$. These field lines maps show that in the disturbed area it is possible to distinguish two different states, noted High (H) and Low (L) levels. On the H level, at a given "t" time, the very large majority of the flux establishes between the orifices, whereas on the L level it establishes on the external sides of the orifices. Of course, this flux distribution is inverted at t+T/2. Moreover, the decrease of the cross section given to the flux circulation is the reason of a decrease of μ_r in this area, and thus the origin of the increase of the reluctance of the MC.

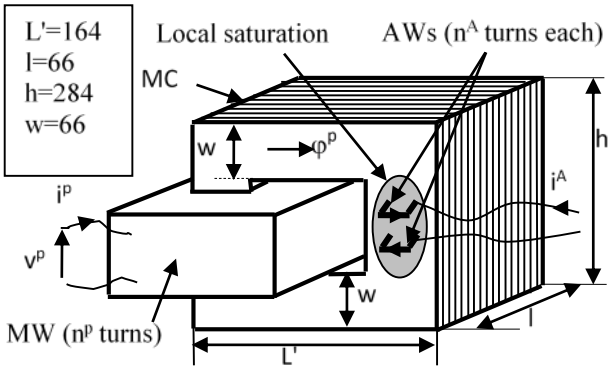

Fig. 1: MC with VAG

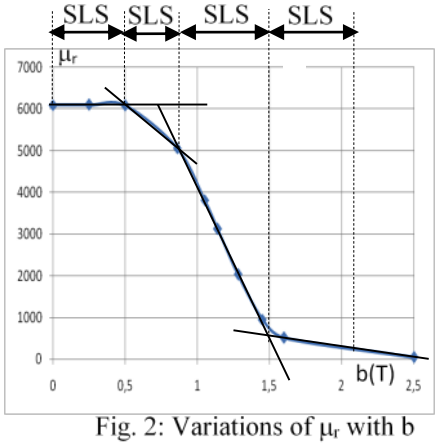

Fig. 2: Variations of μ_r with b

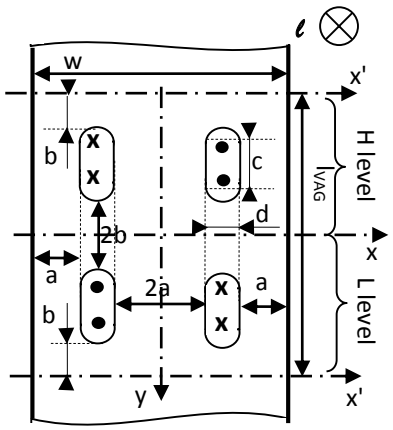

Fig. 3: VAG orifice

(a) : i^A = 20A, i^p = 0A

(b) : i^A = 20A, i^p = 2.18A

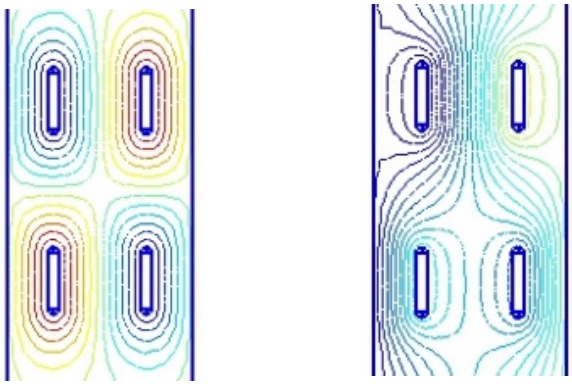

Fig. 4: Magnetic Field line distribution

Analytical modeling of the structure

This modeling is based on the definition of a reluctance network (RN), presented in Fig. 5. $\varepsilon^p=n^p i^p$ and $\varepsilon^A=n^A i^A$ denote the magnetic excitations produced by the MW and AWs respectively, and the signs "+" and "-" associated to ε^A refer to the magnetic opposition previously stated. k_A, associated with ε^A (Fig. 5), is a coefficient allowing to take into account the Ampere-turns losses along the horizontal (x direction) path of the magnetic flux around the orifices. Its minimal value, which should be close to 1, can be computed, as a first approximation, thanks to the following relation:

$$k_A = \frac{b(b+c)}{b(b+c)+a(a+d)} \quad (1)$$

The reluctances R_{MCUA}, R_{int} and R_{ext} refer to the undisturbed MC area, to the area located inside and on the external sides of an AWs respectively (Figs. 3 and 5). Given the symmetries of the device, R_{int} and R_{ext} are defined each with a section equal to $2\ell a$ and a height equal to $l_{VAG}/2=2b+c+d$. Considering that the reluctances presenting different heights from those of the orifices allows to take into account the distortion appearing on the field lines at the extremity of the orifices, as shown in Fig. 4. Actually, it has been noted, by using FEA, that the magnetic potential difference along x' is negligible when x' is located at a distance b of the extremity of an orifice (Fig. 3). Finally, to use this RN, the curve $\mu_r(b)$ has been linearized by portions (Fig. 2). For a k straight line segment (SLS_k), the relative permeability is defined by:

$$\mu_r = \alpha_k + \beta_k b \text{ for } b_{min\,k} < b < b_{max\,k} \quad (2)$$

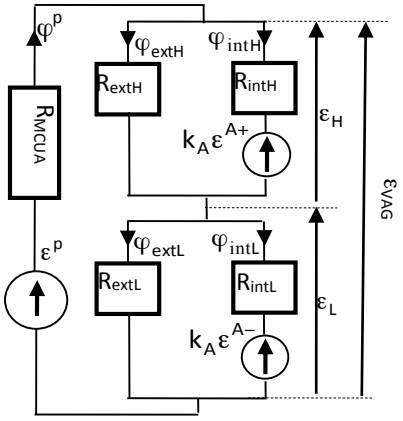

Fig. 5: Reluctance network

Table 1 gives the values of α_k and β_k with respect to "k":

	α_k	β_k	b_{min}	b_{max}
k=1	6050	100	0	0.5
k=2	7627.75	-3055.55	0.5	0.86
k=3	10830.5	-6779.66	0.86	1.517
k=4	1372.55	-545.02	1,517	2,1

Table 1 : Characterization of $\mu_r(b)$ by segments

At a given v^p, *i.e.* given φ^p and given $b^p = \varphi^p / S_{MC}$, the distribution of the magnetic flux in the VAG areas is unknown. Considering the rule of flux conservation and the areas related to the H level, by assuming that the operating points located between and on the sides of the orifices belong to a k and a k' portion respectively, the equation to solve is:

$$(N_1-K_A i^A D_1) b_{intH}^2 + (N_2-K_A i^A D_2) b_{intH} + (N_3-K_A i^A D_3) = 0 \quad (3)$$

By introducing the vacuum permeability μ_0, the parameters in relation (3) can be defined as follows:

$$K_A = 2\mu_0 k_A n^A / l_{VAG} \tag{4}$$

$$\left.\begin{aligned} N_1 &= 2a(\beta_{k'} - \beta_k) \\ N_2 &= -2a(\alpha_k + \alpha_{k'}) + b^p w(\beta_k - \beta_{k'}) \\ N_3 &= b^p w \alpha_k \\ D_1 &= -2a\beta_k\beta_{k'} \\ D_2 &= 2a(\alpha_{k'}\beta_k - \alpha_k\beta_{k'}) + \beta_k\beta_{k'}b^p w \\ D_3 &= \alpha_k(2a\alpha_{k'} + \beta_{k'}b^p w) \end{aligned}\right\} \tag{5}$$

Setting:

$$\Delta = (N_2 - K_A i^A D_2)^2 - 4(N_1 - K_A i^A D_1)(N_3 - K_A i^A D_3) \tag{6}$$

leads to :

$$b_{intH} = \frac{-(N_2 - K_A i^A D_2) \pm \sqrt{\Delta}}{2(N_1 - K_A i^A D_1)} \tag{7}$$

Hence, the rule of flux conservation allows to compute b_{extH} with: $b_{extH}=b'^p-b_{intH}$ where b'^p is the magnetic flux density for $i^A=0$ in the reduced area through orifices: $b'^p=b^p w/2a$.
Then, one has to check if the resulting b_{intH} and b_{extH} quantities belong to the intervals delimiting the k and k' portions according to relation (2) and table 1. If not, another couple [k,k'] is chosen and the procedure is performed again until relevant values are found. Then, the same procedure is performed for the L level.

Waveforms

• The study presented in previous sections leads to the following equalities:

$$\left.\begin{aligned} R_{intH} &= R_{extL} \\ R_{extH} &= R_{intL} \end{aligned}\right\} \tag{8}$$

Which can also be written in terms of induction:

$$\left.\begin{aligned} b_{intH} &= b_{extL} \\ b_{extH} &= b_{intL} \end{aligned}\right\} \tag{9}$$

• Fig. 6a shows the variations, during one period of the supply voltage, of $\delta v^p = v^p / \hat{v}^p$, b^p and i^p for i^A=20 A and $v^p = V^p\sqrt{2}\cos(\omega t)$ with V^p=240 V and f=50 Hz. By comparison, this figure also shows the vairations of i_0^p, *i.e.* i^p when i^A=0 A. Fig. 6b, as for it, shows the variations, during the same period, of the magnetic potential differences ε_H, ε_L and ε_{VAG}. It can be noted that the FEA of the device leads to almost identical results. Implicitly, it validates the expression of k_A given by relation (1) as well as the fact that the Ampere-turns losses at the extremity of the orifices, given the chosen geometry, are negligible.

Note that the presented waveforms can be qualified as « theoretical » either for the proposed analytical model or for the FEA. Indeed, in both cases, the effects of the resistance of the MW are not taken into account, in one hand, and i^A is an absolutely perfect DC current, *i.e.* the AWs are supplied by ideal sources. Moreover, the curves shown in Fig. 6 attest the efficiency of the VAG, especially on the amplitude variations of i^p compared to i_0^p.

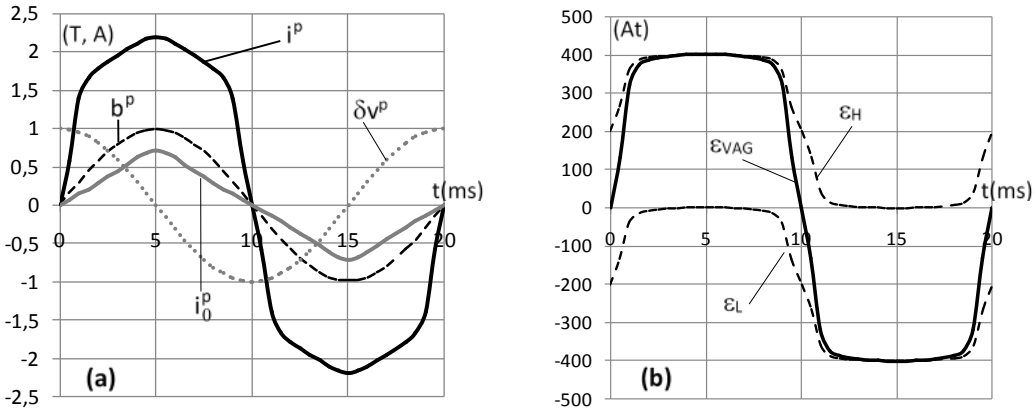

Fig. 6: variations with them of: **(a)** δv^p, b^p, i^p, i_0^p - **(b)** ε_H, ε_L, ε_{VAG} for V^p=240 V and i^A=20 A

Fig. 6b highlights that ε_{VAG} is almost equal to $n^A i^A$ and $-n^A i^A$ when $b^p>0$ and $b^p<0$ respectively. Then, it is possible, as a first approximation, to characterize the VAG by the following relation:

$$n^p i^p = R_{MCUA}\varphi^p + n^A i^A \mathrm{sgn}(\varphi^p) \tag{10}$$

Assuming l_{VAG} negligible with respect to L_{MC}, it is then possible to express relation (10) as follows:

$$n^p i^p = n^p i_0^p + n^A i^A \,\mathrm{sgn}(\varphi^p) \tag{11}$$

Fig. 7a presents the variations with respect to time of b'^p (which is equal to b^p up to a constant), of b_{intH} and b_{extH}. The relations describing the behavior of the MW, its own resistance being neglected, can be written : $v^p = \frac{d\psi^p}{dt}$, where ψ^p denotes the flux embraced by these windings. The leakage flux also being neglected, this flux is $\psi^p=n^p\varphi^p$. Moreover, since $\varphi^p=n^p i^p/R_{MC}$, where R_{MC} is the MC reluctance, it is possible to evaluate the instantaneous value of the inductance $L^p=n^{p2}/R_{MC}$. Then, obtaining the value of "g" (thickness of the equivalent mechanical air gap) can be performed by comparing the value of φ^p with φ_0^p, where φ_0^p is φ^p for i^A=0. Now, denoting R_{MC0} the value of R_{MC} for i^A=0 and assuming that $g<<L_{MC}$ lead to the relations: $R_{MC}=R_{MC0}+R_g$ where R_g is the reluctance of the equivalent mechanical air gap of thickness "g". Then, the value of g can be deduced:

$$g = \mu_0 S_{MC} R_g \tag{12}$$

Fig. 7b shows the variations of L^p, L_0^p and "g" with respect to time during one period of the supply voltage. Moreover, $b^p(t)$ is also shown in Fig. 7b in order to better find the position of the extrema of the deduced quantities. Note that those quantities present quite disturbed variations that do not allow an easy pre-designing phase. Moreover, it also shows that the VAG counteracts the natural effects of the saturation, which leads to a decrease of L^p for i^A=0.

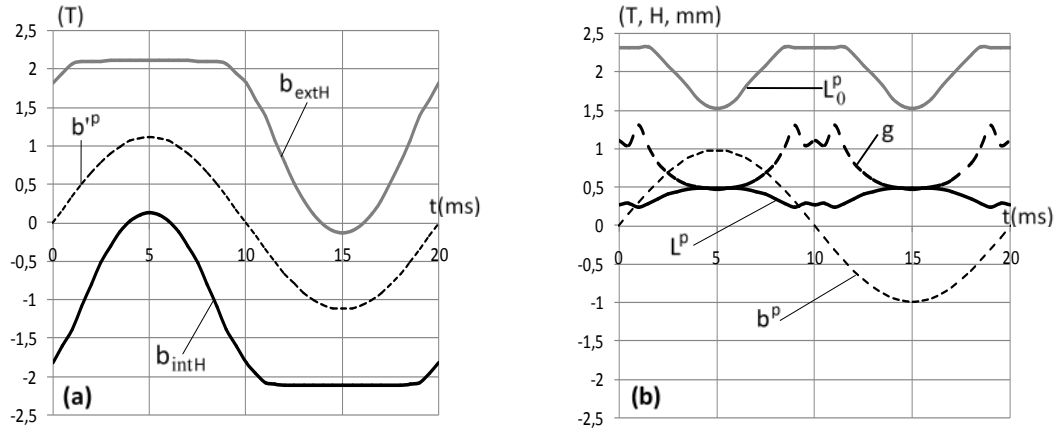

Fig. 7: Variations with time of : **(a)** b'^p, b_{intH}, b_{extH} – **(b)** b^p, g, L^p, L_0^p for V^p=240 V, i^A=20 A

Characteristics and experimental checks

In order to propose a more suitable designing tool allowing to proceed to reliable experimental validations, the sinusoidal currents associated with the real currents will be used. To this end, the fundamental component of those currents as well as the concept of equivalent sinusoidal current, which is widely used in the study of transformers, can be considered. By definition, we associate with the R.M.S. value of a disturbed current a sinusoidal current presenting the same R.M.S. value. Now, considering the case previously described, which leads to Figs. 6 and 7, the peak value $\hat{i}_{(1)}^p$ of the fundamental component of i^p is: $\hat{i}_{(1)}^p$=2.455 A . The R.M.S. value I^p of i^p is: I^p=1.7667 A , leading to a peak value of the equivalent sinusoidal current $\hat{i}_{(rms)}^p$ equal to 2.498 A. About i_0^p , the computed values are: $\hat{i}_{0(1)}^p$=0.606 A and $\hat{i}_{0(rms)}^p$=0.611 A . Then, the difference between the peak values of the fundamental component and the equivalent current is less than 2% for i^p and around 1% for i_0^p . Then, the errors made by using the equivalent sinusoidal currents are compatible with the assumptions made to perform this analytical study, considering that the main aim of this quantity is about the experimental aspect.

Now, since only sinusoidal quantities are considered, the relations previously stated for the determination of the instantaneous values of L^p and "g" lead to characterize those quantities by their mean values $<L^p>$ and <g>. Then, by definition, they present a constant value during a period of the voltage supply:

$$\left.\begin{aligned} <L^p> &= \frac{\hat{v}^p}{\hat{i}_{(1)}^p w} \\ <g> &= m_0 S_{MC} n^{p2} \frac{w}{\hat{v}^p}[\hat{i}_{(1)}^p - \hat{i}_{0(1)}^p] \end{aligned}\right\} \qquad (13)$$

Relations (13) are defined in terms of fundamental component of the currents. To use the concept of equivalent sinusoidal current, $\hat{i}_{(1)}^p$ and $\hat{i}_{0(1)}^p$ have to be replaced by $\hat{i}_{(rms)}^p$ and $\hat{i}_{0(rms)}^p$ respectively.

Fig. 8 shows the variations of $<L^p>$ (Fig. 8a) and <g> (Fig. 8b) for several values of V^p. In order to cover the entire range of the characteristic curve $\mu_r(b)$, the values of V^p are chosen such that, for i^A=0 and $b^p=\hat{b}^p$, the operating point is:

- approximatively in the middle of section 1: V^p=70 V , $\hat{b}^p \approx$0.3 T ,
- approximatively in the middle of section 2: V^p=170 V , $\hat{b}^p \approx$0.7 T ,
- on the upper level of section 3: V^p=240 V , $\hat{b}^p \approx$1 T ,
- on the lower level of section 3: V^p=330 V , $\hat{b}^p \approx$1.35 T ,

- approximatively in the middle of section 4 : V^p=430 V , $\hat{b}^p \approx 1.8$ T .

The surface of an orifice being 80 mm^2, and since n^A=20, the surface of a wire of the AW is 4 mm^2. By setting the permissible current density to 5 A/mm^2, the maximum value for i^A is 20 A, which means that for i^A>20 A, the values of <L^p> and <g> cannot be taken into account and require a new design of the structure.
Fig. 8 shows that the variations of <L^p> are quite complex, whereas the variations of <g> are smooth. Fig. 8b shows the efficiency of the VAG by highlighting that the performances in terms of equivalent air gap thickness increase with i^A, and decrease with V^p. This result was expected since for high values of V^p the saturation affects the whole magnetic circuit.

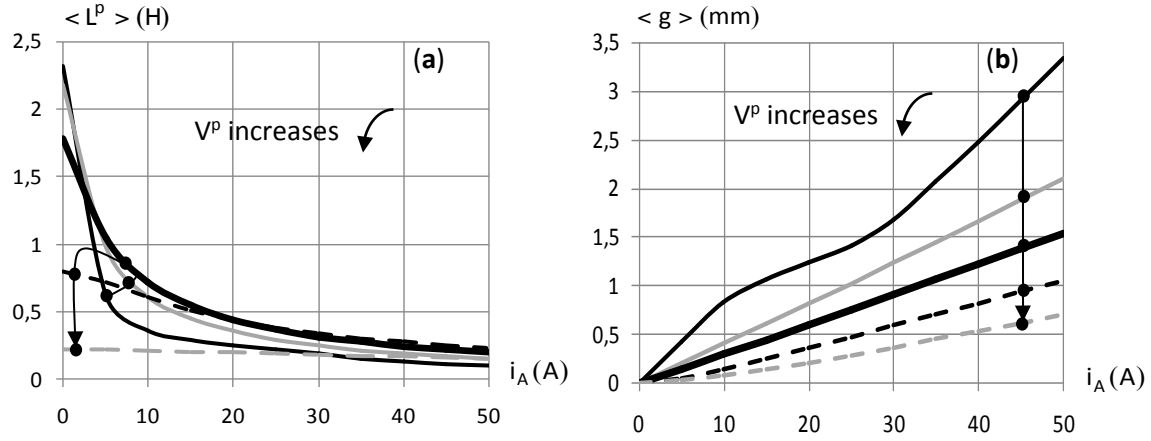

Fig. 8: Variations with i^A of: - **(a)** < L^p > , **(b)** < g > ,
parameter V^p (V^p=70V, 170V, 240V, 330V and 430V)

A prototype of such a structure, which will be used as an inrush current limiter [5], is being built. Then, in this paper, experimental measurements about <g> are reversed from several papers already published. Fig. 9, reversed from [8], is about a very similar magnetic structure with circular orifices. Nevertheless, this MC comes with two VAG instead of one. Then, the results presented in [8] must be divided by a coefficient, which is almost 2, in order to be compared to the ones presented in Fig. 8b. Moreover, Fig. 9 shows the variations of <g> with respect to i^A for several values of V^p (30V, 55V, 110V and 220V), as well as the results of a finite element analysis.
It can be noted that despite the differences between the two structures, the results given by the analytical model presented in this paper are in good accordance with those using the concept of equivalent sinusoidal current. This is indeed remarkable since, from an experimental point of view, the assumptions made about the MW resistance and the ideal current sources are no longer satisfied. Since those elements affect the waveforms of the currents and the flux, it appears that the concept of equivalent sinusoidal current dims the distortions in those quantities.
In order to make a rigorous comparison, the proposed model has been used at V^p=220 V. Fig. 10 shows the variations of <g> with respect to i^A, considering only one VAG. In this figure, <g> is obtained experimentally (Exp.), by the reluctance network proposed in this paper (RN), by a FEA and by Eq. 14. Indeed, relations (13) and (11) lead to an approached value of <g>:

$$<g> = m_0 S_{MC} n^p n^A \frac{w}{\hat{V}^p} i^A \qquad (14)$$

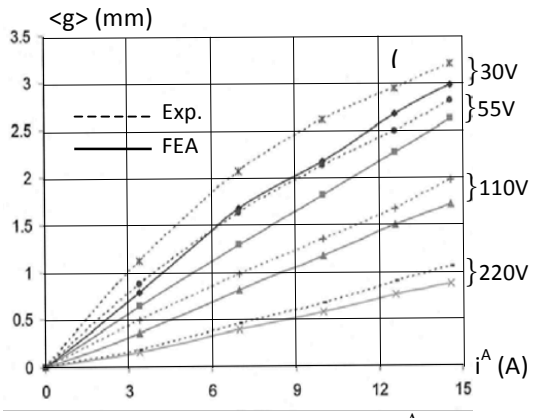

Fig. 9: Variations of <g> with i^A for various V^P voltages

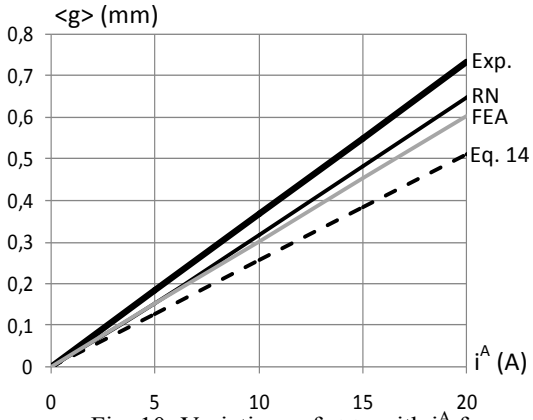

Fig. 10: Variations of <g> with i^A for V^P=220V and different characteristic

It appears that all the methods underestimate the value of <g>. Moreover, the maximum difference between the Exp. and Eq.14 curves is up to 30%, for i^A=20 A, whereas the results given by the reluctance network method are in good accordance with the experimental measurements. Then, if the aim of a study is to quickly obtain a first sizing, then one can use relation (14). If the study needs more accuracy, then the reluctance network should be used.

Conclusion

The purpose of this study is to propose a pre-designing tool of a device including a VAG in order to be able to quickly answer to questions such as: What is the impact of the shape of the orifices on the results ? What is the impact of the electrical steel grade on the performances of the VAG ? In the case of using grain oriented electrical steel, is it better to use the rolling direction or the transverse direction ? Of course, the questions depend on the application, but the authors think that the developed spreadsheet is a suitable tool to answer those questions in the case of a single-phase structure, keeping in mind that sometimes additional finite element computations can be required in order to improve the results.

Note that this step has to be supplemented in order to obtain a full designing tool for a three-phase structure, which introduces an additional complexity to the problem due to the imbalance occurring in the magnetic cores when they each include a VAG.

BIBLIOGRAPHIE

[1] V. Molcrette *et al*: "Reduction of inrush current in single phase transformer using virtual air gap technique". IEEE Trans. on Magnetics, Vol. 34, N°4, July 98, pp. 1192-1194.

[2] S. Magdaleno and C. Rojas, "Control of the magnetizing characteristics of a toroidal core using virtual gap," in Electronics, Robotics and Automotive Mechanics Conference (CERMA), Sep. 2010, pp. 540–545.

[3] J. AvilaMontes, E. Melgoza: "Scaling the virtual air-gap principle to high voltage large power applications". Electrical Machines (ICEM), XXth Intern. Conference on, Sep. 2012, pp. 757–762.

[4] A. Konrad, J.F. Brudny: "An improved method for virtual air gap length computation". IEEE Trans. on Magnetics, Vol. 41, N° 10, Oct. 2005, pp. 4051-4053.

[5] J.F. Brudny, P. Guuinic, V. Costan: "Series current limiter using a magnetic circuit comprising holes and windows". Patent N° WO/2012/126886, sept. 2012.

[6] P. Guuinic, J.F. Brudny, V. Costan, M. Dessoude. "Series voltage regulator with electronics protected against short-circuits by magnetic circuit-based decoupling using holes and windows". Patent N° WO/2012/126884, sept. 2012.

[7] V. Majchrzak, G. Parent, J.F. Brudny, V. Costan and P. Guuinic. "Coupling transformer with a virtual air gap for the protection of dynamic voltage restorers", in the 40th Annual Conference of the IEEE Industrial Electronics Society (IECON 2014), Nov. 2014, pp. 462-468.

[8] A. Konrad, J.F. Brudny. "Virtual air gap length computation with the finite element method". IEEE Trans. on Magnetics, Avril 2007, Vol. 43, pp. 1829-1832.